



# Virtual Methodology for Active Force Cancellation in Automotive Application Using Mass Imbalance & Centrifugal Force Generation (CFG) Principle

**Abhishek Paul** FCA US LLC

**Michael Latcha** Oakland University

**Citation:** Paul, A. and Latcha, M., "Virtual Methodology for Active Force Cancellation in Automotive Application Using Mass Imbalance & Centrifugal Force Generation (CFG) Principle," SAE Technical Paper 2024-01-2343, 2024, doi:10.4271/2024-01-2343.

Received: 24 Oct 2023

Revised: 23 Jan 2024

Accepted: 24 Jan 2024

## Abstract

A variety of structures resonate when they are excited by external forces at, or near, their natural frequencies. This can lead to high deformation which may cause damage to the integrity of the structure. There have been many applications of external devices to dampen the effects of this excitation, such as tuned mass dampers or both semi-active and active dampers, which have been implemented in buildings, bridges, and other large structures. One of the active cancellation methods uses centrifugal forces generated by the rotation of an

unbalanced mass. These forces help to counter the external excitation force coming into the structure. This research focuses on active force cancellation using centrifugal forces (CFG) due to mass imbalance and provides a virtual solution to simulate and predict the forces required to cancel external excitation to an automotive structure. This research tries to address the challenges to miniaturize the CFG model for a body-on-frame truck. The virtual tool presented in this paper will help predict the maximum amplitude cancellation at resonance for given imbalance mass and frequency of forced excitation.

## 1. Introduction

In the past there have been many techniques developed to reduce vibrations or dissipate energy in a system to improve comfort, design, durability, and product life. These techniques have been utilized and implemented in many engineering disciplines such as civil, aerospace, marine and vehicle. Most of these techniques rely on mass damping or force cancellation. With the advent of new technologies, active control has become very popular in various industry applications. Active control monitors and excites the state variables of a system to achieve vibration reduction, typically using mass dampers or force cancelling actuators during the operation cycle of the structure. For example, when an engine is operating, the acoustic vibrations coming from the engine can be reduced by generating forces with equal amplitude and opposite phase which cancel out the noise. This can be done by building a closed loop controller which can modify the feedback based on the input of the system within milliseconds. In addition, the state space system can have an imbalance mass which can rotate and create an equal and opposite force to counter the forcing function. This can be done directly by controlling the imbalance mass rotation and using it in a feed-forward loop by predicting the response

before the output or by a feedback loop by studying the response output and then generating an appropriate function to counter the forces and reduce output. Road shake issues have been common in automotive industry and many countermeasures have been identified to tackle this issue. When a vehicle goes over a bump or rides over a pothole, then forces are transmitted from the tires into the knuckle and the spindle which then transmits the forces into the body directly in case of unibody vehicles or through the frame in case of body on frame vehicles. Suspension bushing and shock tuning is thereby critical to manage road excitations and provide relief for a good ride performance. In some cases, the forcing frequency of the road input excites the suspension hop or tramp modes which may align with the global bending or torsion frequency of the body or frame. This leads to resonance and amplifies the vibration amplitudes which is felt by the driver or the passengers in vehicle. The motivation behind this study and development of this tool comes from a field issue on a body on frame truck where the suspension hop mode aligns with the bending frequency of the frame resulting in resonance and a vertical shake issue. This degrades the ride performance and causes discomfort to the driver and the passengers in vehicle.

## 2. Review of Existing Methods

In this section the existing methods of damping are illustrated. Mass dampers essentially work on the principle that an added mass-spring-damper system will help reduce the amplitudes of resonance of the exciting force and natural mode of a system, or to move the natural modes of a system away from the exciting frequency. A tuned mass damper (TMD) is configured to resonate at a particular frequency. When that frequency is excited by an external force, the tuned mass damper resonates out of phase with the structural motion, hence dissipating the energy [1]. Tuned mass dampers have been used in many applications such as crankshaft torsional dampers, steering wheel torsional dampers etc. In another paper [2], a simulation model of a centrifugal pendulum absorber has been presented which has been analyzed to reduce vibrations within the drivetrain. The author [2] provides a list of limitations to the simulation model, such as Coriolis forces are neglected, only torsional vibrations have been considered, only one vehicle configuration with a single gear and 6 cylinders have been used for simulation etc. In the above-mentioned study, the author placed masses on rollers on either side of a flywheel at an offset from the carrier. The carriers have cutout paths on which the rollers move so that the masses act as pendulums. When the flywheel is connected to the gearbox and engine, centrifugal forces are generated from the rotation of these pendulum masses at different velocities and are used to regulate unwanted torsional vibrations originating from the firing pulses of the engine [2]. The author considered epicycloidal paths for the rollers to induce tautochronous motion, that is, the same oscillatory frequency through the range of amplitudes [3]. The author [2] illustrated a multi-body dynamics model for the flywheel subsystem and used a scripting software to define the epicycloidal curved path which the pendulum masses follow during the drivetrain simulation. The centrifugal forces produced with these masses are directed towards the center of flywheel which helps counter the incoming torsional vibrations. The author [2] concludes by listing the limitations of the simulation model and describes areas for improvement. The future work recommended includes improvement in the centrifugal pendulum absorber geometry by including cutouts, end-stops, rollers, mirrored masses etc.

Application and development of semi-active dampers have been presented in [4]. A numerical method to build semi active dampers to control the appropriate tuning of tuned mass dampers has been discussed. This model has been developed to be applied in bridges to control/dampen the lateral vibrations of long suspension bridges. The initial numerical model is built using a simple 2 degree of freedom system, the 1<sup>st</sup> degree of freedom representing the structure and the other degree of freedom representing the tuned mass damper. An additional damper is placed in the system between the structure and TMD which has a control switch. The model works

on the principle that when the velocity of the TMD and the displacement of the structure are in same phase then the control of the semi-active damper remains off and when they are not in opposite phase then the control is switched on which then allows the semi-active damper to either create impulses causing a phase lead or locking the mass of the TMD causing a phase lag [4]. Author [4], has also presented numerical modelling of semi-active dampers for multi degree of freedom structures. This principle has been used to model the MDOF system for this paper as a starting point.

Active mass dampers have been developed for slender structures, high-rise buildings, bridges, and automotive vehicles. It works on the principle of accelerating masses to generate inertial forces, with a control loop to regulate this movement and dampen input vibrations. One such application has been presented in [5]. In this paper, the author has presented the working principle and development of an active mass damper for bridges. The focus of the paper is on the lateral vibration reduction of bridges due to pedestrians, and the flutter control of a bridge deck section. Author has also presented a test setup to validate the functioning of the developed active mass damper. The rotating mass unbalance presented in [2] is the main principle used for developing the virtual force cancellation technique presented in [3]. These forces can be controlled by the number of unbalanced rotating masses [5]. In the rotating unbalanced mass system presented in the paper, the system relies on the fact that there are two actuators on both sides of the device with masses attached to a rod which rotates with same angular frequency in the opposite direction. The centrifugal force generated is the sum of two vertical forces as the horizontal components cancel out each other. An assumption here is that the rod connecting the mass to the actuator is massless. The author [5] also illustrates that the direction of the generated centrifugal force can be manipulated by changing the relative position between the left and right rotors. The paper also mentions the additional moments created in the model and how they can be eliminated to generate pure horizontal control forces. The author describes combinations of damper units for various applications.

In another paper [6], authors have theoretically modeled an active mass damper with negative acceleration feedback control of single degree of freedom structure, shown theoretically and experimentally through the application of the NAF [6] control algorithm to reduce vibrations in multi degree of freedom structures. The authors have used AC servo motors controlled by PID controller to control the movement of the active masses. A multi-input and multi-output feedback control for vibration suppression in buildings has also been proposed in [7]. The authors have modeled a negative acceleration feedback control to support multiple accelerometers and multiple active mass dampers. This has also been validated theoretically and experimentally using a 2-story building like structure [7]. Chang and Yang [8] have also presented a closed loop control system to control vibrations in building structures modeled as a SDOF system.

Active tuned mass damper with velocity feedback and complete feedback has been presented in the paper [8].

Samali and Al-Dawod [9], have presented a five-story benchmark model with active tuned mass damper controlled by a fuzzy control. The advantage of fuzzy controller being its ability to handle nonlinear behavior and robustness. The authors have also compared active control between a fuzzy controller and a LQR controller. The benchmark model has been analyzed under earthquake excitations. In conclusion from the research study, it was found that response reduction using fuzzy controllers is comparable and, in some case, better than LQR controller although one needs to have good knowledge base and an expert understanding of fuzzy logic to build the control system [9]. Active control of coupled structures has been demonstrated in [10]. Acceleration feedback control and DC servo motor have been used to design and validate the control system developed [10]. H2/LQG approach has been implemented to design the control strategy and minimize accelerations in both building structures under seismic excitations. In another paper [11], active mass dampers have been modeled using rotating actuators. A mathematical model has been derived to suppress vibrations in SDOF system due to external excitations. In this paper [11], Lagrange equations have been used to derive the system of equations and hierarchical sliding mode controller has been presented to control the state variables. Numerical and experimental analysis has been performed to validate the model and reduce vibrations in the system due to external excitations. Vertical vibrations in the system are neglected as they are deemed to negligible in comparison with the horizontal vibrations in the system presented in the paper [11]. The forces generated by an actuator in an ATMD controlled by linear quadratic Gaussian controller has been presented by Young-Moon Kim et.al. [12]. The authors have presented a composite tuned mass damper controlled using LQG controller to minimize vibrations due to wind responses in tall buildings. A composite tuned mass damper consists of both passive and active tuned mass dampers which are used to suppress the vibrations in a structure. In control theory, optimal control is deduced when all states of the system and output are a combination of all the states [12]. Due to the random nature of the wind induced vibrations, the input and output are a function of random vibrations with a constant power spectral density of Gaussian white noise and an observer is modeled to estimate all the state variables of the system. LQG controller is used to define the system of equations and state variables in which the linear dynamic system is a function of Gaussian white noise with constant power spectral density. An active hybrid control, which is a combination of an active tuned mass damper and base isolation has been presented in [13]. A proportional integral derivative (PID) controller with negative feedback error closed loop has been used to control the system under earthquake excitations. The required control forces are computed using feedback error which is calculated as the difference between desired response and actual output [13]. A simulation model has also been presented in the

paper. In addition, a few more articles related to control system design and its application in automotive structures have been researched. [16], highlights the use of active disturbance rejection control to mitigate vibrations in electric drive systems of electric vehicles. The authors focus on vibrations due to impact such as potholes and bumps and reducing them with use of active disturbance rejection and electric current compensation. The electric current compensation helps in managing the sudden changes in the motor current during impact. A set of data on electric drive system response with and without the active vibration control has been presented. Stabilization of the current variation using current compensation technique has also been demonstrated. The design and construction of car's body and the perception of vehicle dynamics felt by the occupant has been presented in [17]. Experimental studies conducted on the car's body and drivers' response to driving on various road surfaces have been presented. The authors observed that certain frequencies and amplitudes of vibrations were more strongly associated with specific driving characteristics, such as acceleration, braking, and cornering. Study concluded that low frequency range vibrations from 4-8 Hz were influential in determining the driver's perception of the driving dynamics. The paper suggests that by reducing or modifying specific vibrations, manufacturers may be able to create a more desirable driving sensation that aligns with the intended performance characteristics of the vehicle. Overall, the article highlights the role of feelable structure vibrations in shaping the perceived driving dynamics and emphasizes the potential for car manufacturers to leverage these insights to improve the overall driving experience for their customers.

Derrix, D. and Prokop, G. [18], have investigated the impact of body stiffness on the drivability and dynamic behavior of a vehicle through on-road experiments. The authors observed that higher body stiffness was associated with improved steering response, increased stability, and reduced body roll during cornering. On the other hand, lower body stiffness resulted in a more comfortable ride but potentially compromised the vehicle's handling and responsiveness. The paper concluded with highlighting the importance of finding an optimal balance between comfort and performance when it comes to adjusting body stiffness.

### 3. Proposed Method

Even though physical prototypes have been built in large-scale, small-scale units for implementation in cars is new and limited. The control system designed to control this system is proprietary to the corporations building these products. Therefore, limiting the application of these products in vehicles as physical prototypes. Also as mentioned above, majority of the research has been done in civil structures with rectilinear actuators. Different control algorithms have also been researched in past to control the systems and state variable each having their

advantages and disadvantages. Having a control system design integrated with finite element modelling will help build a virtual tool which can be used as a directional/predictive tool to aid in vehicle product development and suppress vibrations in automotive structures. The objective of this research is to research active force cancellation techniques and develop a virtual tool which works on the force cancellation technique using centrifugal force generation with imbalance mass and provide a directional input to the engineers to identify the percentage of amplitude reduction for the vertical shake issue for a given imbalance weight and eccentricity. This knowledge helps the automotive engineers to determine a packaging scope of an Active CFG and the weight penalty to the program for a percentage improvement in ride performance. The proposed research also shows the working principle and characteristics of a DC motors which are used in this system to drive the actuators used to generate the cancellation forces. This is essential to understand the equations used in the simulation model blocks of the tool to define the cancellation force actuator. Finally, a study to identify the optimum location for the tool has also been presented showing the results for different locations.

### 3.1. DC Motors

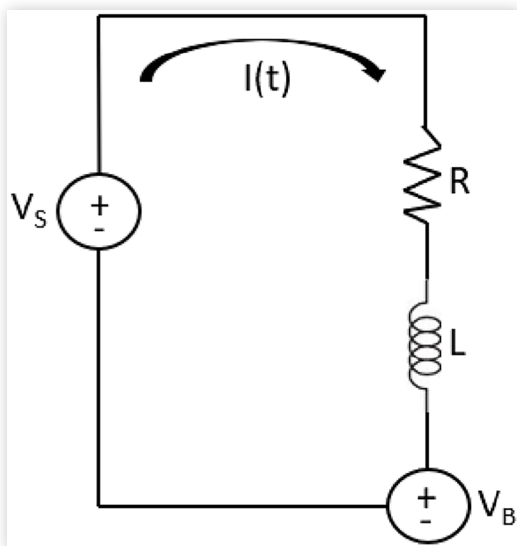
Figure 1 shows a circuit containing current, resistance, inductance, source voltage and back EMF voltage.

$$V_s = R * i(t) + L * \frac{d(i(t))}{dt} + V_B \quad (1)$$

$V_s$  is source voltage,  $R$  is armature resistance,  $i(t)$  is current at given time,  $L$  is armature inductance and  $V_B$  is back EMF.

$$V_B = \omega * K_B \quad (2)$$

**FIGURE 1** Electrical Circuit



$\omega$  is rotation velocity of the shaft and  $K_B$  is back EMF constant.

$$T = J * \dot{\omega} \quad (3)$$

$T$  is Motor Torque,  $J$  is Moment of Inertia and  $\dot{\omega}$  is rotational acceleration

$$T = K_T * i(t) \quad (4)$$

$K_T$  is motor torque constant  
From equations (3) and (4),

$$K_T * i(t) = J * \dot{\omega}(t) \quad (5)$$

From equations (1) and (2),

$$V_s = R * i(t) + L * \frac{d(i(t))}{dt} + (K_B * \omega(t)) \quad (6)$$

From equation (5),

$$\dot{\omega}(t) = \frac{K_T * i(t)}{J} \quad (7)$$

From equation (6),

$$\frac{d(i(t))}{dt} = \frac{V_s - R * i(t) - (K_B * \omega(t))}{L} \quad (8)$$

Integrating equations (7) and (8) with Initial Condition = 0 over time period,

$$\omega(t) = \omega(0) + \frac{K_T}{J} * \int (i(t)) dt \quad (9)$$

And

$$i(t) = i(0) + \frac{1}{L} * \int \{V_s - R * i(t) - (K_B * \omega(t))\} \quad (10)$$

$$\omega(0) = 0 \text{ and } i(0) = 0$$

From equation (10),  $\omega$  varying with time has been calculated for a given current varying with time, source voltage, resistance, inductance and constant  $K_B$ .

However, the above set of equations represent a theoretical DC motor than a practical DC motor as friction is assumed to be 0. Next, the equations for a more practical DC motor which includes friction have been derived.

$$T - (B_f * \omega) = J * \dot{\omega} \quad (11)$$

Where,  $B_f$  is the rotational friction damping coefficient.

From equations (4) and (11),

$$K_T * i(t) - (B_f * \omega) = J * \dot{\omega}(t) \quad (12)$$

Assuming for now,  $K_T = K_B = K$

Therefore [equations \(6\)](#) and [\(12\)](#) can be written as

$$V_s = R * i(t) + L * \frac{d(i(t))}{dt} + (K * \omega(t)) \quad (13)$$

$$K * i(t) - (B_f * \omega(t)) = J * \dot{\omega}(t) \quad (14)$$

Taking Laplace of [equations \(13\)](#) and [\(14\)](#)

$$V_s - R * I(s) - L * s * I(s) - (K * s * \theta(s)) = 0 \quad (15)$$

$$K * I(s) - (B_f * s * \theta(s)) = J * s^2 * \theta(s) \quad (16)$$

$I(s)$  and  $s * \theta(s)$  are Laplace transform of  $i(t)$  and  $\omega(t)$  respectively and initial conditions are considered to be 0.

From [equation \(16\)](#),

$$I(s) = \frac{(s * \theta(s)) * (J * s + B_f)}{K} \quad (17)$$

Substituting [equation \(17\)](#) in [equation \(15\)](#) and since  $s * \theta(s) = \dot{\theta}(s)$ ,

$$V_s = \left\{ \frac{(L * s + R) * (J * s + B_f)}{K} + K \right\} * \dot{\theta}(s) \quad (18)$$

Which gives,

$$\frac{V_s}{\dot{\theta}(s)} = \left\{ \frac{(L * s + R) * (J * s + B_f)}{K} + K \right\} \quad (19)$$

This can be rewritten as,

$$\frac{\dot{\theta}(s)}{V_s} = \left\{ \frac{K}{(L * s + R) * (J * s + B_f) + K^2} \right\} \quad (20)$$

Assuming  $i$  and  $\omega$  as state variable,

$$\dot{\theta} = K / J * i - \frac{B_f}{J} * \omega = \frac{d\omega}{dt} \quad (21)$$

And,

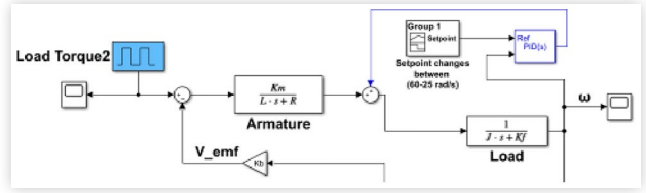
$$\frac{di}{dt} = \frac{V_s}{L} - \frac{R}{L} * i - \frac{K}{L} * \omega \quad (22)$$

This can be written in state space form as,

$$\frac{d}{dt} \begin{bmatrix} \omega \\ i \end{bmatrix} = \begin{bmatrix} -\frac{B_f}{J} & \frac{K}{J} \\ -\frac{K}{L} & -\frac{R}{L} \end{bmatrix} * \begin{bmatrix} \omega \\ i \end{bmatrix} + \begin{bmatrix} 0 \\ \frac{1}{L} \end{bmatrix} * V_s \quad (23)$$

This can now be represented in the simulation model as shown in [Figure 2](#).

**FIGURE 2** Representation of the DC motor.



## 3.2. CFG Working Principle

In this section, the fundamental principle on which the force cancellation is based on has been discussed. One must define mass imbalance and dynamic behavior of a system under the influence of mass imbalance. An imbalance mass  $m_2$  is introduced and the lumped mass as  $m_1$  is assumed which is located at a distance of  $e$  which is termed as eccentricity. [Figure 3](#) describes the system. [Figure 4](#) describes the free body diagram of the system. From this system the equation of motion can be derived as following,

A single degree of freedom (SDOF) system consists of lumped mass  $m$ , spring stiffness  $k$  and damper  $c$ . Force  $f$  is applied to the right-hand side of the system and equation of motion can be defined and acceleration, velocity and displacement can be computed as following,

$$m\ddot{x}(t) + c\dot{x}(t) + kx(t) = f(t) \quad (24)$$

**FIGURE 3** SDOF System with Unbalanced Mass

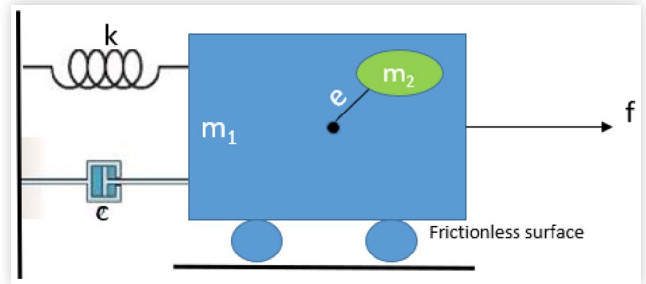
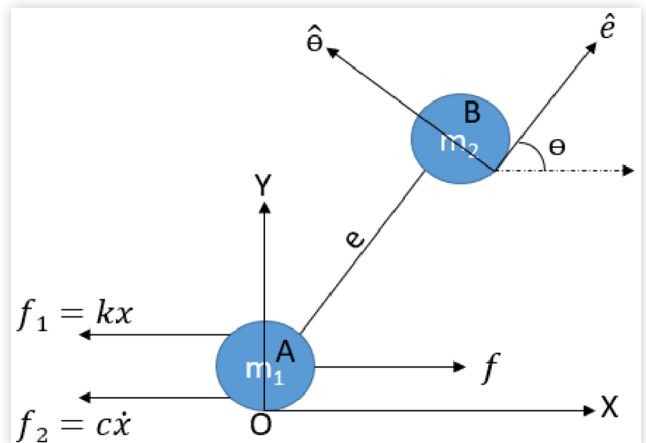


**FIGURE 4** Free Body Diagram



Which gives,

$$\ddot{x}(t) = (f(t) - c\dot{x}(t) - kx(t)) / m \quad (25)$$

Where  $\ddot{x}(t)$  is the acceleration,  $\dot{x}(t)$  is the velocity and  $x(t)$  is the displacement of the lumped mass under forced excitation  $f(t)$ . Applying Newton's second law to the SDOF system with mass imbalance,

$$\Sigma F = m_2 * \overline{a_{B/O}} = m_2 * \overline{a_{A/O}} + m_2 * \overline{a_{B/A}} \quad (26)$$

$$\Rightarrow m_2 \ddot{x} + m_2 \left[ (\ddot{e} - e\dot{\theta}^2) \hat{e} + (e\ddot{\theta} + 2\dot{e}\dot{\theta}) \hat{\theta} \right] \quad (27)$$

where  $\dot{e} = \ddot{e} = 0$  since arm length does not change over time and  $\dot{\theta} = \ddot{\theta}$  which is a constant.

$$\Rightarrow m_2 \ddot{x} \hat{i} - m_2 e \dot{\theta}^2 \hat{e} \Rightarrow \hat{e} = \text{Cos}\omega t \hat{i} + \text{Sin}\omega t \hat{j} \quad (28)$$

$$\Rightarrow m_2 \ddot{x} \hat{i} - m_2 e \omega^2 (\text{Cos}\omega t \hat{i} + \text{Sin}\omega t \hat{j}) + m_2 g \hat{j} \quad (29)$$

Resolving in X and Y components,

$$\Sigma F_{m_{2x}} = m_2 \ddot{x} - m_2 e \omega^2 \text{Cos}\omega t = \Sigma F_{m_{1x}} \quad (30)$$

$$\Sigma F_{m_{2y}} = -m_2 e \omega^2 \text{Sin}\omega t + m_2 g \quad (31)$$

Since one is interested in the X direction only for this paper, this can further used as

$$\Sigma F_{m_{1x}} = m_1 \ddot{x} = -\Sigma F_{m_{2x}} = -m_2 \ddot{x} + m_2 e \omega^2 \text{Cos}\omega t \quad (32)$$

Which gives,

$$(m_1 + m_2) \ddot{x} = m_2 e \omega^2 \text{Cos}\omega t \quad (33)$$

Considering the forces due to the damper and spring from [Figure 3](#), [equation \(33\)](#) can be rewritten as

$$(m_1 + m_2) \ddot{x} = m_2 e \omega^2 \text{Cos}\omega t - kx - c\dot{x} \quad (34)$$

Note,  $m_2 e \omega^2 \text{Cos}\omega t$  is the centrifugal force whose direction depends on the rotational direction of the imbalanced mass. In this paper, it is used to provide counter force to the external force to reduce acceleration, velocity, and displacement of the system.

## 4. Virtual Model – SDOF System

In this section the Single degree of freedom system and its definition in a virtual simulation model and its behavior under external force excitation has been discussed. Force

cancellation using the force actuator definition and how the accelerations, velocities and displacements can be cancelled for an ideal system (no losses) has also been illustrated. The equations and findings from the previous section to define a virtual simulation model consisting of a SDOF system with external force excitation and a DC motor with a PID controller to feed into a force actuator used to cancel the external force in real time have also been shown. [Figure 5](#) shows a single degree of freedom representation in simulation model. To cancel an unit force excitation, equal and opposite force is introduced into the system. [Figure 6](#) shows calculation of equal and opposite force based on the output response from the single degree of freedom system which is fed back into the system to cancel the initial force. The phase lag error between the excitation force and cancellation force is controlled using a PID controller. This is the most simplistic representation of force cancellation in theory and is shown in [Figure 7](#).

The actuator represents the physics of centrifugal force generation using imbalance mass. The difference in response output measured in terms of acceleration when the actuator is switched off and the response output when it is switched on has been compared. Learnings from sections described earlier have been applied in this section to come up with this virtual tool. Some of the key differences between what is represented in this section vs the model described above is the use of a DC motor to generate the angular velocity used by the centrifugal force actuator to generate the cancellation force and create a closed loop system which helps in reducing the response output for a given force excitation to a SDOF system. Using these learnings from one can represent the SDOF system with the mass imbalance in state space form as following,

Assuming the same system described in [Figure 3](#) for which the equation of motion is described in [equation \(34\)](#). Therefore, in state space form,

**FIGURE 5** SDOF System

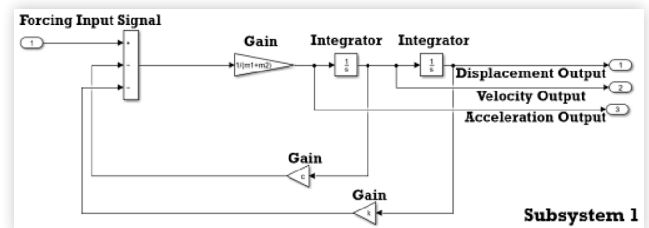


**FIGURE 6** Cancellation Force representation

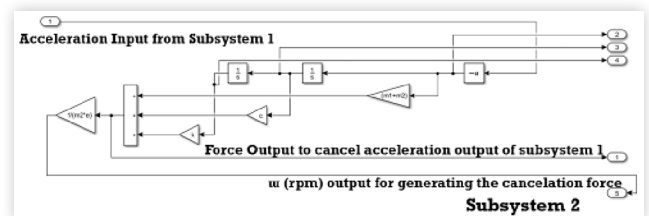
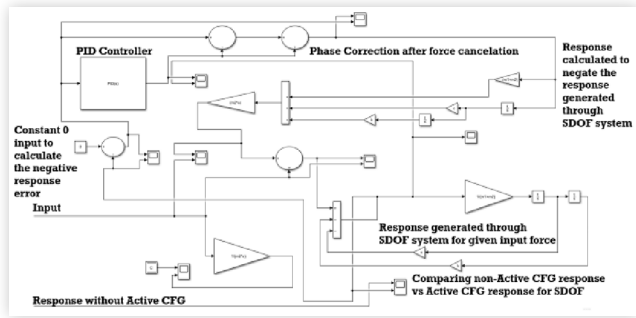


**FIGURE 7** Force Cancellation for ideal SDOF using PID Controller



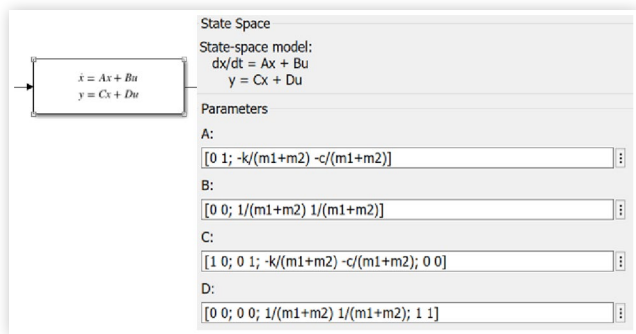
$$\dot{x} = Ax + Bu; y = Cx + Du \quad (35)$$

Where,

$$A = \begin{bmatrix} 0 & 1 \\ -k & -c \end{bmatrix}; B = \begin{bmatrix} 0 & 0 \\ 1 & 1 \end{bmatrix}; C = \begin{bmatrix} 1 & 0 \\ 0 & 1 \\ -k & -c \\ 0 & 0 \end{bmatrix}; D = \begin{bmatrix} 0 & 0 \\ 0 & 0 \\ 1 & 1 \\ 1 & 1 \end{bmatrix} \quad (36)$$

This can be represented in simulation model using the state space block and filling up the A, B, C and D matrices from equation (36) as shown in figure below.

**FIGURE 8** State Space Form of SDOF System



Next, an input to the system has been defined. This will represent the external excitation of the force into the SDOF system defined in state space. Referencing fundamentals of state space system, it can clearly be seen that from the system defined in equation (36), the B matrix is of dimension 2X2 which means that 2 inputs to the system are required. Out of the 2 inputs, the 1<sup>st</sup> will be the external excitation force and the 2<sup>nd</sup> will be the actuation force coming from the centrifugal force generator which will be defined ahead. This would be the cancellation force

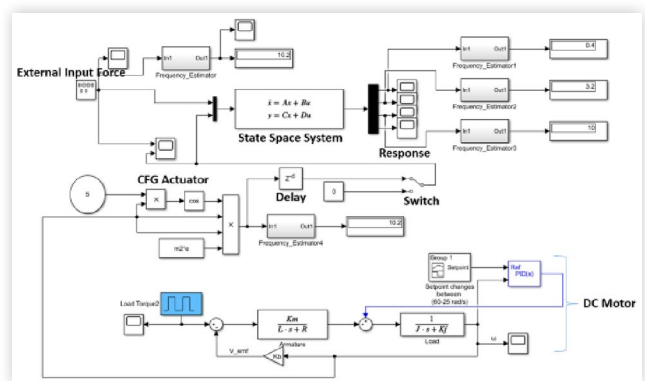
used to cancel the external force to reduce the response of the system. Prior to this the state space system being excited by an external force has been tested to see if it correctly generated the desired output. For now, the 2<sup>nd</sup> input has been kept zero the state space system has been excited with a sinusoidal input of 10 Hz and amplitude of 1000 N. For this test, mass  $m_1 = 200$  Kgs,  $m_2 = 0.2$  Kgs,  $k = 1000$  N/mm and  $c = 3.8$  Ns/mm have been assumed. After validating the system, the next step is to define a block to measure the frequency of excitation and a DC motor as described in section 3.1. In addition, an actuator has also been defined which will take the angular velocity generated from the DC motor output shaft to then generate a force which will eventually become the cancellation force. The PID controller inside the DC motor will help control the angular velocity of the shaft based on input voltage and load torque.

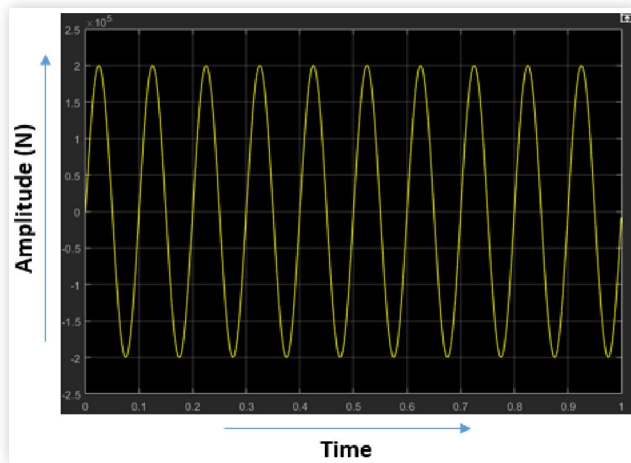
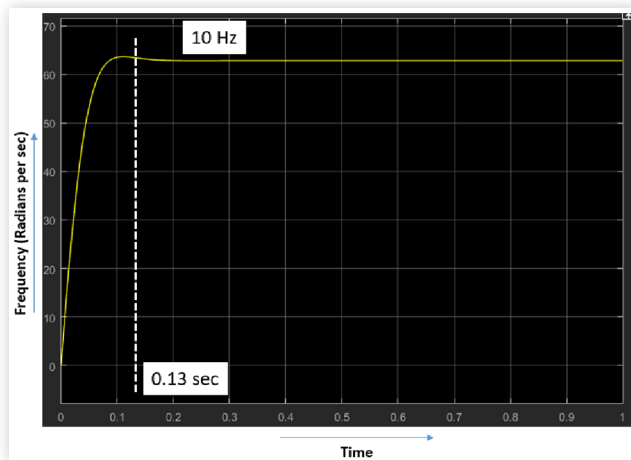
A PID controller could have been used directly to control the output response from the system and generate a signal to cancel the excitation but that would not serve the practical purpose as in reality an external motor with an actuator is needed to generate the force that can reduce the response from the system. Figure 9, shows the system with DC motor, CFG actuator and frequency counter added to the system.

The tool also includes a switch to see the response with and without the cancellation force coming through the CFG actuator. For test, an external force excitation has been added in form of a sinusoidal wave of amplitude 1 KN and frequency of 10 Hz shown in Figure 10. The simulation is run for 1 second and since for a given motor torque is proportional to current and back emf is proportional to rpm therefore a standard DC motor has been used with following numerical values of the coefficients.  $L = 0.5$  Henrys,  $R = 2$  Ohms,  $K_f = 0.2$  Nms,  $K_b = 0.1$ ,  $J = 0.02$  Kgm<sup>2</sup>/s<sup>2</sup> and  $K_m = 0.1$ .

The switch is turned on at 0.07 seconds and the actuator supplies the cancellation force generated from the angular velocity achieved for the DC motor used. Figure 11 shows the time taken by the DC motor to achieve 10 Hz speed which is equivalent to 60 rps. It takes about 0.13 seconds to achieve a steady state of the velocity. The maximum centrifugal force generated for given mass and eccentricity and this angular velocity is

**FIGURE 9** SDOF Active CFG Virtual Tool



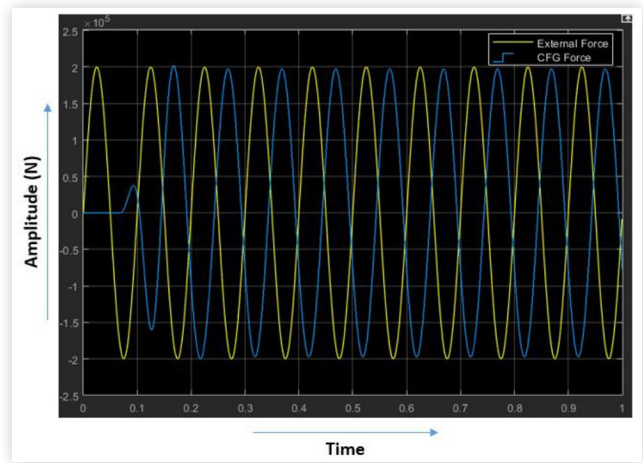
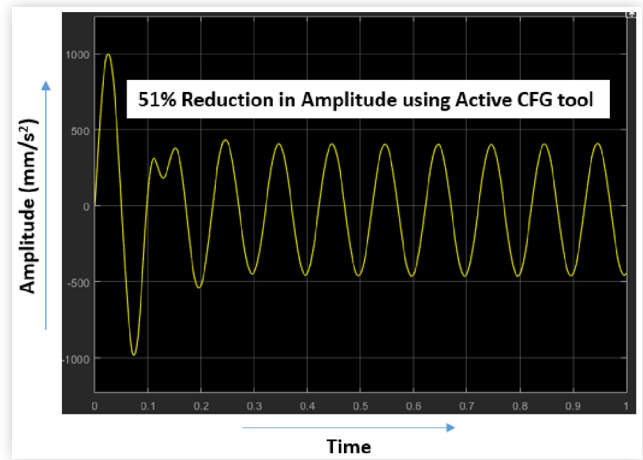
**FIGURE 10** Sinusoidal Excitation Force**FIGURE 11** Angular Velocity Output from DC Motor Controlled by PID

about 1 kN. Due to the time taken by the DC motor to achieve steady state, there is a slight difference in frequency of the CFG force and the external force and since this is a transient analysis, some cancellation to reduce the acceleration response is expected but not complete 0 and the force reduction from the force output through the system has also been checked.

Figure 12, shows a comparison of the external force with the CFG cancellation force which starts its maximum amplitude at about 0.13 seconds as it is proportional to the time taken by the DC motor to reach its steady state velocity of the shaft.

Figure 13 shows the acceleration response when the CFG is switch on. A reduction in the response output and the force has been observed.

For complete cancellation the time taken by the DC motor to achieve the steady state needs to be minimized thereby reducing the difference in frequency between the excitation force and the CFG force. Theoretically if the frequency is identical then the cancellation will be 100% but, there will be some loss due to time lag required for achieving steady state of the velocity. This can be optimized further to improve performance by tuning the PID controller

**FIGURE 12** Excitation Force vs CFG Cancellation Force**FIGURE 13** Acceleration Response Output with Amplitude Reduction

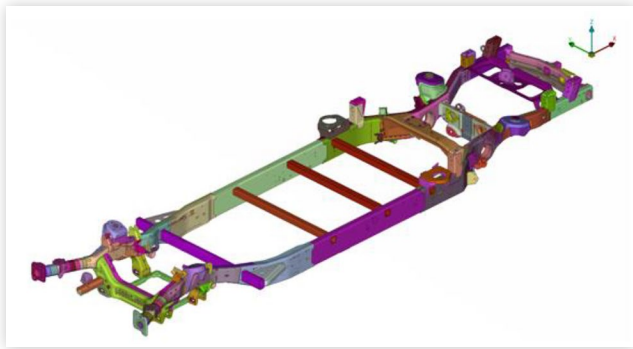
better but for this test it was not done as the objective was to see if the tool is performing the cancellation to reduce the output through the system which it did achieve.

In the next sections, a deep dive into MDOF system has been shown starting with defining a truck frame and illustrating the state space model of the frame using finite elements, scripting and FEM. Use of the virtual tool to simulate and cancel responses for this truck frame has also been shown.

## 5. Virtual Tool Validation for A Truck Frame

With the learnings from all the previous sections, a state space model for a full vehicle truck frame with multiple degree of freedom has been defined in this section. The first step in this is to model a finite element model of a 169-inch wheelbase truck frame. Figure 14 shows the finite element model of the truck frame. After model checks, the first step is to run the normal mode analysis to determine the first bending mode of the frame. A full vehicle

**FIGURE 14** Finite Element Frame Model



issue has been identified in this vehicle which was a vertical shake issue which has been observed at around 8.5 Hz at a full vehicle level. This is primarily due to high amplitudes above the target due to the vertical bending mode of the full vehicle which at frame level is noted to be at around 19.7 Hz and therefore the objective has been defined to reduce the output acceleration amplitude at the bending node of the first bending mode of the frame. To work with this problem without making it computationally expensive the full vehicle has been stripped down to frame level without any trims and the issue has been addressed at this stage. The finite element model has a total of 156271 elements. Total mass of the frame is 295 Kgs. The model details and degradation concerns have been summarized in [Table 1](#) below. The frame is excited at the suspension location in Z direction to induce bending mode and the CFG is placed at the center node of the frame cross member to cancel/reduce the maximum amplitude for the bending mode. [Figure 15](#) shows this configuration and the location of the force excitation, Active CFG location and the response output measurement point. This model is then converted to modal domain to reduce computational time and the mass, stiffness, damping and force matrices have been extracted using DMAP in FEM software. This is then represented in state space format and modal superposition has been used to compute the response with the Active cancellation switched OFF and then switch ON at about 0.4 seconds. The simulation is run for 2 seconds. [Figure 16](#) shows the time taken by the

**TABLE 1** FE Model & Issue Summary

<b>Mode Size</b>	<b>156271</b>
<b>Weight</b>	<b>295 Kgs</b>
<b>Issue</b>	<b>Vertical Shake</b>
<b>Problem Frequency in Vehicle</b>	<b>8.5 Hz</b>
<b>Bending Mode - Full Vehicle</b>	<b>8 Hz</b>
<b>Bending Mode - Frame</b>	<b>19.7 Hz</b>

**FIGURE 15** Loading, Response and Active CFG Locations

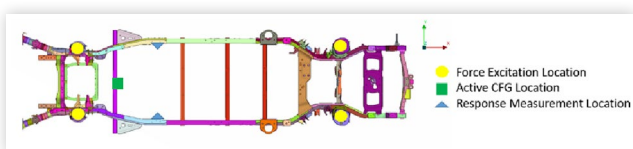
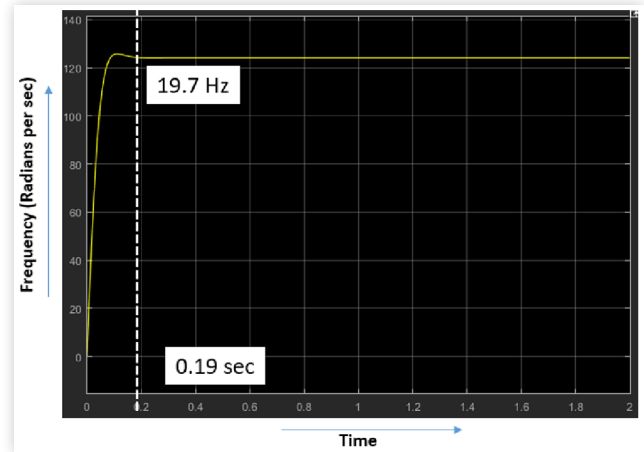


**FIGURE 16** Angular Velocity Output from DC Motor Controlled by PID

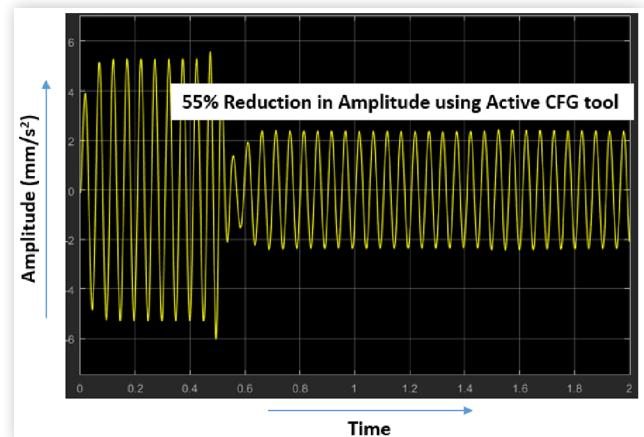


PID controller to control the required angular velocity and stabilize it. [Figure 17](#) shows the amplitude reduction once the Active cancellation is switch ON.

A sinusoidal excitation force of 10 KN is introduced to the system to excite the truck frame at the bending frequency of 19.7 Hz. The imbalance mass is assumed to be 2Kgs for the truck frame weighing at 295 Kgs. The eccentricity is assumed to be 250mm. [Figure 17](#) also depicts when the Active CFG tool is switched OFF initially, the acceleration output is high and after it is switched on at about 0.4 seconds, it then takes about 0.2 seconds for the PID controller to stabilize the angular velocity of the output shaft in the DC motor. Following this the amplitude reduction of about 55% is observed in the acceleration response output.

Following this a study has been conducted to identify the optimized location of the virtual tool which would provide the maximum amplitude reduction. To identify this location, multiple locations were selected based on the packaging constraints of the program. [Figure 18](#) shows 9 locations that were initially identified. The reduced mass, stiffness and damping matrices were extracted from FEM using DMAP for all the 9 locations and the state space system representing each of the 9 iterations were created using scripting.

**FIGURE 17** Acceleration Output Reduction Using Active CFG Tool



The response amplitude improvement and the stabilization time for the controller have been presented in a bar chart format as seen in Figure 19. Figure 20 shows the acceleration output reduction location 4. In addition, it has been observed that placing the ACFG tool in any location may not show positive reduction and based on the mode shape and the load path may result in negatively impacting the performance as shown in locations 3, 5 and 6. Also the time take by the controller to stabilize the angular velocity of the DC motor to compute the cancellation force from the actuator varies. As seen in Figure 19, the least time taken for stabilization is at location 6 but it negatively impacts the performance. The next best solution from the stabilization perspective is for location 7 which shows about 37% amplitude

**FIGURE 18** Loading, Response and Active CFG Points for Optimum Location Identification

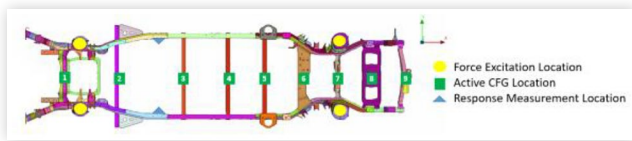


**FIGURE 19** Response Amplitude Improvement & Stabilisation Time Chart

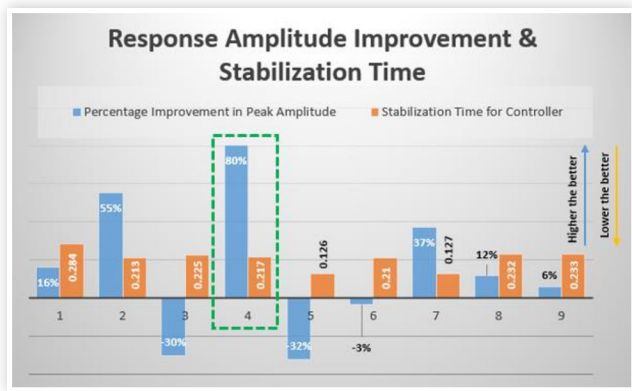
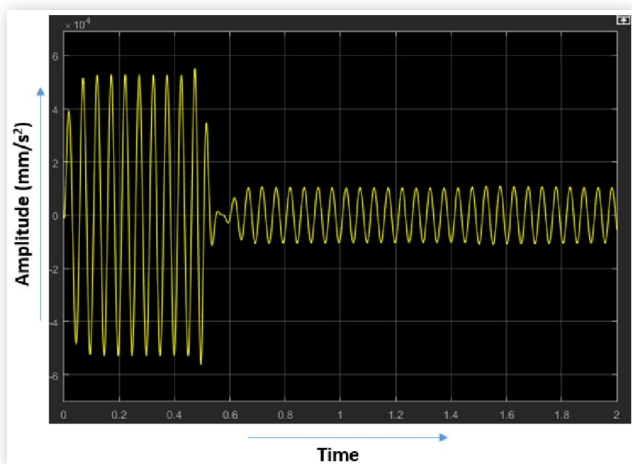


**FIGURE 20** Acceleration Output Reduction Using Active CFG Tool for Location 4



reduction. This highlights a requirement to have a balance between the amplitude reduction improvement and the time taken to get this improvement. This tool helps the engineers to plan the design of the structure and use of ACFG more accurately and answer the questions related to how much improvement can be achieved virtually for a given imbalance mass, eccentricity and DC motor properties and finding the most optimum location prior to constructing a physical prototype.

## 6. Conclusions

In conclusion fundamental principles of mass imbalance and DC motors have been presented and a SDOF system representation has been shown in the simulation model. A virtual tool for active force cancellation using CFG principle has been demonstrated and its successful implementation for a SDOF system has been shown.

It has been concluded that the frequency of the excitation force needs to match the angular velocity of the DC motor shaft for effective cancellation. Additional observations showed that minor phase lag between the excitation and cancellation forces result in cyclical reduction and amplification of the final output, therefore an additional inclusion of error correction was deemed necessary for consistent reduction without any amplification of the final output. The study also concluded that for a given imbalance mass and eccentricity which is limited due to product cost, weight and size requirements, only partial reduction of final output response can be achieved instead of 100% negation of the amplitudes which is only possible theoretically but not practical for the actual program.

A finite element model of a truck frame has been built and reduced in modal domain and represented in simulation model by extracting the mass, stiffness, damping, eigenvalue, displacement and force matrices using DMAP from FEM and scripting. It has been observed that solving the system of equations for the finite element model in physical domain is computationally very expensive as the matrices were huge, therefore reduction of the model using eigenvalues in modal domain helps reduce the computation time significantly without compromising on the accuracy of the solution. Successful demonstration of amplitude reduction for a truck frame at the bending frequency has been shown using the Active CFG tool and modal super position principle. This study helped in identification of the imbalance mass and designing the physical prototype required for achieving required percentage reduction in the output response for vertical shake issue presented in the vehicle.

Finally, an optimum location for placing the ACFG tool has been shown highlighting the percentage of amplitude reduction improvement and time taken for the controller to stabilize the angular velocity of the motor shaft for actuation for given imbalance mass, eccentricity and DC motor properties. This helped in designing the fixture and identifying the best package and manufacture feasible location to place the physical prototype on the frame.

## References

- Intro to Structural Motion Control – Tuned Mass Damper Systems, College of Engineering Purdue.
- Smith, E., “Analysis and Simulation of Centrifugal Pendulum Vibration Absorbers,” Royal Institute of Technology.
- Alsuwaiyan, A. and Shaw, S., “Performance and Dynamic Stability of General-Path Centrifugal Pendulum Vibration Absorbers,” *Journal of Sound and Vibration* 252, no. 5 (2002): 791-815.
- Ferreira, F., Moutinho, C., Cunha, A., and Caetano, E., “Use of Semi-Active Tuned Mass Dampers to Control Footbridges Subjected to Synchronous Lateral Excitation,” *Journal of Sound and Vibration* 446 (2019): 176-194.
- Scheller, J., and Starossek, U., “A Versatile Active Mass Damper for Structural Vibration Control,” Structural Analysis and Steel Structures Institute, Hamburg University of Technology.
- Yang, D.H., Shin, J.H., Lee, H.W., Kim, S.K. et al., “Active Vibration Control of Structure by Active Mass Damper and Multi-Modal Negative Acceleration Feedback control algorithm,” *Journal of Sound and Vibration* 392 (2017): 18-30.
- Talib, E., Shin, J.H., and Kwak, M.K., “Designing Multi-Input Multi-Output Modal-Space Negative Acceleration Feedback Control for Vibration Suppression of Structures Using Active Mass Dampers,” *Journal of Sound and Vibration* 439 (2019): 77-98.
- Chang, C.C. and Yang, H.T.Y., “Control of Buildings Using Active Tuned Mass Damper,” *J. Eng. Mech.* 121, no. 3 (1995): 355-366.
- Samali, B. and Al-Dawod, M., “Performance of a Five-Storey Benchmark Model Using Active Tuned Mass Damper and Fuzzy Controller,” *Eng. Struct.* 25 (2003): 1597-1610.
- Christenson, R.E., Spencer, B.F. Jr., Hori, N., and Seto, K., “Coupled Building Control Using Acceleration Feedback,” *Computer-Aided Civil. Infrastruct. Eng.* 18 (2003): 4-18.
- Zhang, Y., Li, L., Cheng, B., and Zhang, X., “An Active Mass Damper Using Rotating Actuator for Structural Vibration Control,” *Advances in Mechanical Engineering* (2016).
- Kim, Y.M., You, K.P., You, J.Y., Paek, S.Y. et al., “LQG Control of aAlong-Wind Responses of Tall Building Using Composite Tuned Mass Dampers,” *Key Engineering Materials* 723 (2017): 753-759.
- Djedoui, N., Ounis, A., and Abdeddaim, M., “Active Vibration Control for Base-Isolated Structures Using a PID Controller against Earthquakes,” *International Journal of Engineering Research in Africa* 26 (2016): 99-110.
- Zaccarian, L., “DC Motors: Dynamic Model and Control Techniques.”
- Kreyszig, E., *Advanced Engineering Mathematics*, 9th ed. ()
- Ge, S., Hou, S., Yang, Y., Zhang, Z. et al., “Active Vibration Control of Electric Drive System in Electric Vehicles Based on Active Disturbance Rejection Current Compensation under Impact Conditions,” *SAE Int. J. Veh. Dyn., Stab., and NVH* 7, no. 4 (2023): 513-531, <https://doi.org/10.4271/10-07-04-0033>.
- Roessler, S. and Baier, H., “Car Body Influence on the Perceived Driving Dynamics due to Feelable Structure Vibrations,” *SAE Int. J. Veh. Dyn., Stab., and NVH* 6, no. 3 (2022): 311-331, <https://doi.org/10.4271/10-06-03-0021>.
- Derrix, D. and Prokop, G., “Experimental Analysis of the Influence of Body Stiffness on Drivability and Dynamic Body Behavior with On-Road Experiments,” *SAE Int. J. Veh. Dyn., Stab., and NVH* 6, no. 3 (2022): 283-296, <https://doi.org/10.4271/10-06-03-0019>.

## Contact Information

For any question/concerns, contact **Abhishek Paul**.  
[abhishek.paul@stellantis.com](mailto:abhishek.paul@stellantis.com)

## Acknowledgement

The authors would like to recognize and appreciate the help and guidance of Syed Haider, Francisco Sturla and Kevin Thomson at FCA US LLC throughout the project.

## Definitions/Abbreviations

- TMD** - Tuned Mass Damper
- CFG** - Centrifugal Force Generator
- ACFG** - Active Centrifugal Force Generator
- MDOF** - Multiple Degrees of Freedom
- SDOF** - Single Degree of Freedom
- ATMD** - Active Tuned Mass Damper
- LQR** - Linear Quadratic Regulator
- LQG** - Linear Quadratic Gaussian
- PID** - Proportional Integral Derivative
- DC** - Direct Current
- EMF** - Electro Magnetic Force
- DMAP** - Direct Matrix Abstraction Program
- FEM** - Finite Element Model
- NAF** - Negative Acceleration Feedback